

令和 3 年 6 月 10 日現在

機関番号：14301

研究種目：研究活動スタート支援

研究期間：2019～2020

課題番号：19K23650

研究課題名(和文) Study of the oxygen-ion mobility in complex metal-oxide materials prepared by topochemical methods

研究課題名(英文) Study of the oxygen-ion mobility in complex metal-oxide materials prepared by topochemical methods

研究代表者

Amano Patino Midori (Estefani) (Amano Patino, Midori (Estefani))

京都大学・化学研究所・特定助教

研究者番号：80849018

交付決定額(研究期間全体)：(直接経費) 2,200,000円

研究成果の概要(和文)：トポケミカル(構造保存)な方法で作成された金属酸化物は、中程度の温度($T < 900$)で酸素イオン伝導を示すことが期待される。本研究では、還元的・酸化的雰囲気での加熱および加圧処理を組み合わせたトポケミカルな反応を用いることでペロブスカイトおよびペロブスカイト関連構造酸化物を作成した。これらの材料では、カチオンや空孔の秩序が大きく異なっている。放射光X線回折と熱重量測定を用いて、これらの物質の詳細な構造変化を解析した結果、温度による酸素放出/取り込みの挙動を明らかにすることに成功した。

研究成果の学術的意義や社会的意義

近年、新しいクリーンエネルギー源や高エネルギー密度の電池の必要性が高まっており、それらの開発のために特に中低温で動作する新しいイオン伝導材料の研究が盛んに行われている。酸素イオン伝導体は、固体酸化物燃料電池(SOFC)などのデバイスに使用されるキーマテリアルである。本研究の成果は、酸素イオン伝導材料のハリエーションを上げ、また、構造的特徴を活かすことで酸素イオン伝導を制御する可能性を示すもので、持続可能な社会を支えるSOFC技術を開発することにも繋がります。

研究成果の概要(英文)：This project investigated the synthesis and characterization of metal-oxide materials prepared by topochemical (structure preserving) methods. The products of topochemical processes often exhibit oxygen-ion conductivity at moderate temperatures ($T < 900$ °C). A series of perovskite and perovskite-related materials were successfully prepared by using a combination of reductive/oxidative atmospheres coupled with heating and pressure treatments. The materials exhibit markedly different types of cation and/or vacancy ordering. Their detailed structure and oxygen release/incorporation behavior as a function of temperature were analyzed by synchrotron X-ray diffraction and thermogravimetric techniques.

研究分野：0502:無機・錯体化学、分析化学、無機材料化学、エネルギー関連化学およびその関連分野

キーワード：Oxygen-ion mobility Perovskite structure Solid state chemistry Topochemical methods Structural study Synchrotron radiation Rietveld refinement

科研費による研究は、研究者の自覚と責任において実施するものです。そのため、研究の実施や研究成果の公表等については、国の要請等に基づくものではなく、その研究成果に関する見解や責任は、研究者個人に帰属します。

1. 研究開始当初の背景 (Background at the beginning of the study)

Clean energy sources, sensors, and high energy density batteries are central for the development of sustainable energy technologies and this has recently increased the drive for research towards new ionic-conducting materials. Within this category, oxygen-ion conductors find use in important devices for the development of sustainable technologies such as solid oxide fuel cells (SOFCs), and membranes for oxygen separation and the conversion of methane to syngas.¹ Given that in the periodic table more than 75% of the elements are metallic in nature, metal oxides continue being the subject of extensive study in the search for new technologically relevant oxygen-ion conductors.

The phenomenon of oxygen-ion conduction results from the movement of oxygen ions through the crystal lattice (the structure of a solid). For a solid material to be a good oxygen-ion conductor, two main requirements need to be met: (i) the crystal lattice must contain unoccupied cavities or sites for the oxygen ions to hop to, and (ii) the energy barrier to the ion-migration process must be small. Metal oxides do not always meet the aforementioned requirements, however, remarkably high oxygen-ion conductivity values (comparable to those observed in liquid electrolytes and at moderate temperatures), have been achieved in oxides with particular types of crystal lattices.²

A synthetic approach to explore materials adopting such structures where the oxygen-ion conductivity takes place at intermediate temperatures ($250 \leq T (^{\circ}\text{C}) \leq 600$ °C in contrast with $T \approx 900$ -1000 °C) was explored. The project focused on metal-oxide phases synthesized by *topochemical* (structure preserving) methods. The products of topochemical reactions can be selected so that the oxygen-ions are particularly mobile.

2. 研究の目的 (Objectives of the study)

In light of the requirements for the crystal lattice of a material to allow oxygen-ion mobility, materials adopting structures related to the perovskite structure ABO_3 are particularly attractive.³ This is because the perovskite structure can accommodate a wide range of ionic species both in the *A* and *B* sites as shown in Fig. 1, where there are two different species both at *A* and *B* sites (the former disordered while the latter ordered). Additionally, a large number of anion vacancies can also be accommodated in the structure. Such features mean that both the energy barrier to oxygen-ion migration (via the chemical flexibility allowed from the combination of *A* and *B* species) and the partial occupation of oxygen sites (from the flexibility towards anion vacancies) can be ‘tuned’ in the structure. As a result, a number of perovskite oxides are observed to be ‘purely’ oxygen-ion conductors, meaning that the level of any other electronic contribution to the total electrical conductivity can be made negligible. Despite the favorable features of the structure, within the perovskite materials investigated to date, only those based on lanthanum gallate (LaGaO_3) are found suitable for ionic-conduction applications (with average operating temperatures of ~ 1000 °C).² Building on the idea of optimizing materials to attain oxygen-ion conductivity at lower temperatures, the purpose of this project was the exploration of the oxygen-ion conductivity in perovskite and perovskite-related materials prepared via topochemical (*i.e.* structure-conserving) methods. In the resulting products from a topochemical reaction, the energy barriers to ion diffusion for the particular mobile species are overcome at lower temperature regimes compared to thermodynamically stable solids. In particular, materials where the oxygen-ions are particularly mobile stand out in the search for solid-state oxygen-ion conductors with tailored functionality for applications in devices such as solid oxide fuel cells (SOFCs), among others.

3. 研究の方法 (Methodology of the study)

A series of perovskite and perovskite-related materials were prepared by using a combination of reductive/oxidative atmospheres coupled with heating and pressure treatments: the *B*-site ordered material LaSrNiRuO_4 and the *A*-site mixed materials $\text{La}_{1-x}\text{Ba}_x\text{MnO}_{3-\delta}$ ($x = 0.25, 0.50$). Each material exhibits different types of cation and/or vacancy orderings.

The detailed structures of the LaSrNiRuO_4 and $\text{La}_{1-x}\text{Ba}_x\text{MnO}_{3-\delta}$ ($x = 0.25, 0.50$) materials were analyzed by synchrotron X-ray diffraction (SXR) data carried collected at the central facilities NSRRC, Taiwan and SPring-8, Japan. The powder samples were packed into silica capillaries. The capillaries were rotated on the omega axis of the diffractometer during the measurements. Variable temperature measurements in the range 25-800 °C were performed by using a heating nozzle and nitrogen flow. The capillaries were not sealed so that the oxygen from air could be incorporated in the powder samples while the structural changes were captured *in situ*. Rietveld profile refinements were performed using the GSAS suite of programs.⁴

For thorough analysis, in conjunction with the SXR data above described, reductive and/or oxidative thermogravimetric analysis (TGA) measurements were carried out. Measurements were performed by

heating the LaSrNiRuO_4 , $\text{La}_{0.75}\text{Ba}_{0.25}\text{MnO}_{3-\delta}$ and $\text{La}_{0.50}\text{Ba}_{0.50}\text{MnO}_{3-\delta}$ powder samples (20 mg) under a reducing or oxidative gas flows. Samples were heated at $2\text{ }^\circ\text{C min}^{-1}$ to $800\text{ }^\circ\text{C}$ while measuring their mass change.

4. 研究成果 (Summary of Research Results / Findings)

Layered oxygen-deficient LaSrNiRuO_4 materials:

Preliminary TGA data collected during oxidation of LaSrNiRuO_4 materials prepared by topochemical methods from both highly cation-ordered and slightly disordered LaSrNiRuO_6 starting phases are shown in Fig. 1. A step-wise incorporation of oxide-ions into the highly cation-ordered LaSrNiRuO_4 samples was observed (Fig. 1a). Such step-wise behavior is absent when a small degree of Ni/Ru disorder is introduced in the LaSrNiRuO_4 structure (Fig. 1b).

One of the possible explanations for the observed step-wise oxygen-ion incorporation behavior, was considered to be the different environments for the oxide-ion in the lattice created by the *B*-site cation ordering. However, further studies were necessary to fully understand these observations.

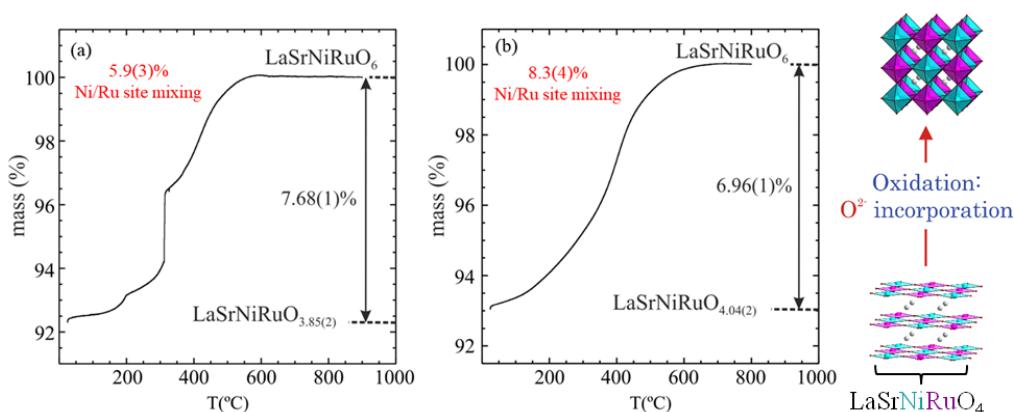


Fig. 1. (a) A stepwise and (b) a smooth oxygen-ion incorporation behavior is observed during oxidation of two LaSrNiRuO_4 samples. The two samples oxidize to LaSrNiRuO_6 and have the same structure but different degrees of cation-ordering between Ni and Ru cations at the *B* sites.

In this project, the incorporation of oxygen in LaSrNiRuO_4 was followed *in situ* by carrying out variable temperature SXR D scans. From these experiments, additional reflections in the diffraction patterns were observed during transformation to LaSrNiRuO_6 (Fig. 2). These reflections were attributed to La_2O_3 , SrO and Ni. These secondary phases are more evident in data collected from LaSrNiRuO_4 materials prepared from slow-cooled LaSrNiRuO_6 starting materials.

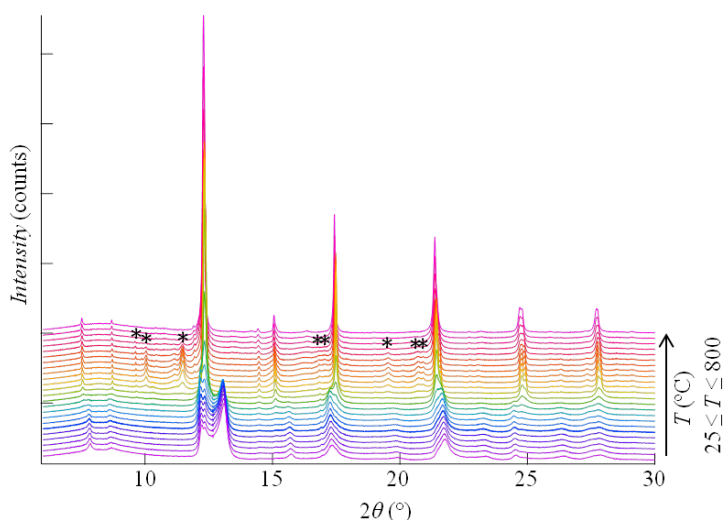


Fig. 2. Additional reflections (marked with the symbol '*') are observed in SXR D patterns collected as a function of temperature, during oxygen incorporation in a highly ordered *B*-site LaSrNiRuO_4 material to form LaSrNiRuO_6 . The additional reflections can be assigned to La_2O_3 , SrO and Ni metal.

Rather than the step-wise behavior for oxygen-ion gain observed in TGA data being a consequence of different environments in the cation-ordered lattice, the non-gradual change from LaSrNiRuO_4 to LaSrNiRuO_6 can be explained from the presence of an increased amount of products of decomposition for samples prepared from slow-cooled starting materials. During preparation of the materials, as the

topochemical reduction of LaSrNiRuO_6 progresses, there is a build-up in the lattice strain from the mismatch in the c lattice parameter between the product LaSrNiRuO_4 and the starting material (the anion deintercalation causes a contraction of the c -lattice parameter from $7.85(1)$ Å to $6.92(1)$ Å, Fig. 3). This strain might cause an increase in the energy barrier for the reduction reaction. In terms of flexibility of particles, the smaller crystalline domains in quenched samples make the particles more ‘plastic’ and the reaction proceeds to completion during formation of LaSrNiRuO_4 . On the other hand, the reduction of slow-cooled LaSrNiRuO_6 samples requires higher temperatures (due to the buildup lattice strain, Fig. 3) which may overcome the energy needed for the competing decomposition reaction yielding small amounts of La_2O_3 , SrO and Ni secondary phases. The differing reactivity of quenched and slow-cooled LaSrNiRuO_6 starting materials indicates that a microstructure comprised of small crystalline domains is required for the topochemical anion deintercalation to form the product LaSrNiRuO_4 under the conditions studied.

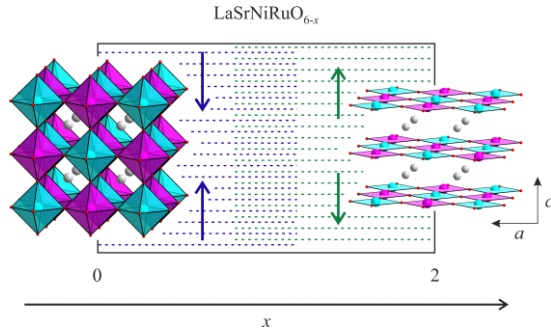


Fig. 3. Representation of the strain ‘regions’ at the reaction interface during reduction of LaSrNiRuO_6 to form LaSrNiRuO_4 . Colored arrows represent the two types of strain generated for x .

Encompassing these results in a broader context, the topochemical preparation of LaSrNiRuO_4 demonstrates that the accessibility of the reduced product via topochemical reduction of some complex transition metal oxide can be limited by the microstructural features of the starting materials. This is in contrast to the reduction of the Ruddlesden-Popper phases $\text{Sr}_2\text{Fe}_{0.5}\text{Ru}_{0.5}\text{O}_4$ and $\text{Sr}_3(\text{Fe}_{0.5}\text{Ru}_{0.5})_2\text{O}_7$ as well as $\text{Y}_2\text{Ti}_2\text{O}_7$, for which chemical or electronic features limit the reactivity of the parent phases towards topochemical reduction. Therefore, the results of this study are relevant for the approach to the preparation of novel topochemical transition metal oxide materials.

$\text{La}_{0.75}\text{Ba}_{0.25}\text{MnO}_{3-\delta}$ and $\text{La}_{0.50}\text{Ba}_{0.50}\text{MnO}_{3-\delta}$ materials:

The crystal structure of $\text{La}_{1-x}\text{Ba}_x\text{MnO}_{3-\delta}$ materials depends on their oxygen content.⁵ In stoichiometric samples of LaMnO_3 , the charge of La is +3, the charge of Mn is +3 and the total positive charge of the two cations is neutralized by three O^{2-} anions per formula unit. In $\text{La}_{1-x}\text{Ba}_x\text{MnO}_{3-\delta}$ the La^{3+} cations are being partially substituted by Ba^{2+} cations, leading to the formation of a fraction of Mn^{4+} for accounting for the charge-imbalance, in turn yielding the formation of oxygen-ion vacancies. $\text{La}_{1-x}\text{Ba}_x\text{MnO}_{3-\delta}$ phases with Mn^{4+} concentrations lower than 12% ($0.05 \leq x < 0.12$) are observed to adopt orthorhombic perovskite structures. Meanwhile the increase of Mn^{4+} concentration (when $x \geq 0.12$) leads to adoption of either the rhombohedral ($R-3c$) or cubic ($Pm3m$) structures. The latter highly symmetric structure normally involves disordered oxygen-vacancy distributions while the rhombohedral case exhibits complex vacancy ordering.⁶ SXRD diffraction data collected from the $\text{La}_{0.75}\text{Ba}_{0.25}\text{MnO}_{3-\delta}$ and $\text{La}_{0.50}\text{Ba}_{0.50}\text{MnO}_{3-\delta}$ materials reveals that the $x = 0.25$ material adopts the $R-3c$ rhombohedral structure while the $x = 0.50$ compound adopts the cubic structure $Pm-3m$ (Fig. 4a).

From variable temperature SXRD data collected from samples contained in capillaries opened to the atmosphere (Fig. 4), the unit-cell volume of the $\text{La}_{0.50}\text{Ba}_{0.50}\text{MnO}_{3-\delta}$ material is observed to increase, as expected from thermal expansion. Meanwhile, a phase transition into a cubic phase is observed at around 700 °C from the originally rhombohedral structure of the $\text{La}_{0.75}\text{Ba}_{0.25}\text{MnO}_{3-\delta}$ material (Fig. 4b). This structural change might be explained from a de-localization of the oxygen-ion vacancies.

Upon cooling back to room temperature, the $\text{La}_{0.75}\text{Ba}_{0.25}\text{MnO}_{3-\delta}$ structure returns to the $R-3c$ rhombohedral symmetry.

From TGA data collected under oxygen flow, for $\text{La}_{0.75}\text{Ba}_{0.25}\text{MnO}_{3-\delta}$ a value of $\delta = 0.13(5)$ can be determined. For $\text{La}_{0.50}\text{Ba}_{0.50}\text{MnO}_{3-\delta}$, $\delta = 0.27(3)$. Thus, the composition of the materials can be written as $\text{La}_{0.75}\text{Ba}_{0.25}\text{MnO}_{2.86(5)}$ and $\text{La}_{0.50}\text{Ba}_{0.50}\text{MnO}_{2.73(3)}$, consistent with the degree of divalent cation-doping at the A sites of each structure. However, for these materials the oxygen stoichiometry cannot be determined from TGA data alone (the oxygen-ion vacancies exhibit a complex equilibrium with the external atmosphere). Therefore, SXRD data is being further analyzed to confirm the Mn^{4+} content (and thus the oxygen content) in the materials. Complementary to these measurements, titrimetric analysis will also be carried out. Topochemical reductions and oxidations are also being performed. Complex broenmillerite-type oxygen-ion vacancy ordering is expected for the reduced phase $\text{La}_{0.75}\text{Ba}_{0.25}\text{MnO}_{2.5}$. The oxygen-ion intake and release behaviour of the cubic and rhombohedral structures will be compared.

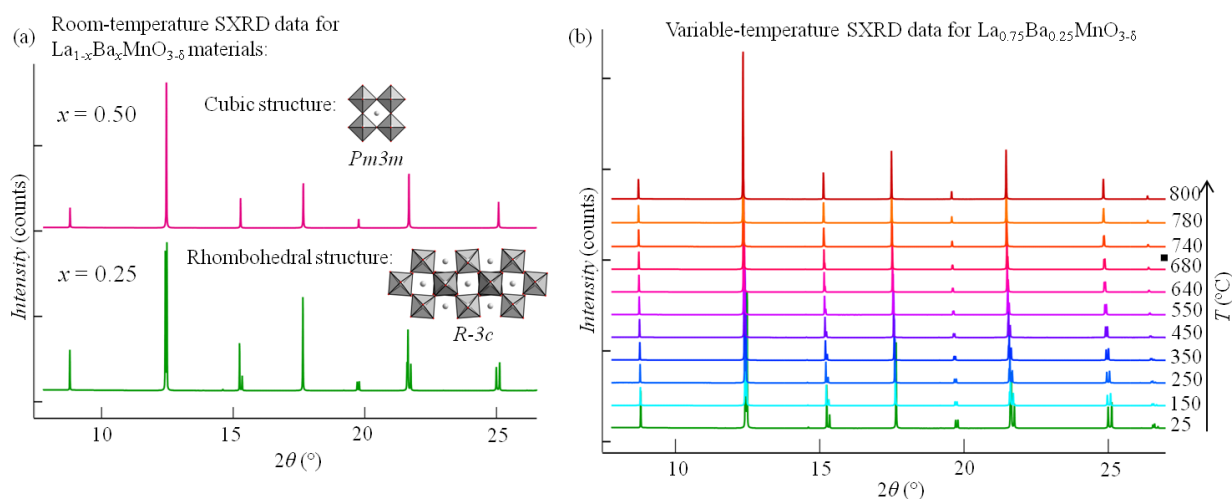


Fig. 4. (a) Room-temperature SXRD patterns for $\text{La}_{0.75}\text{Ba}_{0.25}\text{MnO}_{3-\delta}$ (bottom panel) and $\text{La}_{0.50}\text{Ba}_{0.50}\text{MnO}_{3-\delta}$ (top panel). The latter phase adopts a cubic $Pm\bar{3}m$ structure ($a = 3.99(1) \text{ \AA}$) while $\text{La}_{0.75}\text{Ba}_{0.25}\text{MnO}_{3-\delta}$ adopts the rhombohedral structure $R\bar{3}c$ ($a = 5.54(1) \text{ \AA}$, $c = 13.49(2) \text{ \AA}$). Variable-temperature SXRD for $\text{La}_{0.75}\text{Ba}_{0.25}\text{MnO}_{3-\delta}$ are shown in (b). A transformation from the rhombohedral structure to the cubic $Pm\bar{3}m$ cell is observed from diffraction patterns collected at $T = 680 \text{ }^\circ\text{C}$ (marked with a square '■') and onwards. After cooling, the structure becomes rhombohedral again.

In sum:

Different types of perovskite and perovskite-related materials were successfully prepared by using topochemical methods and their release and incorporation of oxygen-ion behaviour was investigated. The oxygen-ion incorporation behaviour of LaSrNiRuO_4 materials prepared from quenched and slow-cooled LaSrNiRuO_6 starting phases raises awareness towards the microstructural features during topochemical processes.

The results of this research show that accessibility of topochemical products needs to be considered with the microstructural characteristics of the starting materials in mind. This aspect is crucial in the exploration of materials for extending the catalogue of solid-state oxygen-ion conductors with tailored functionality for applications in devices operating at moderate temperatures.

References:

1. Jacobs, R., Mayeshiba, T., Booske, J. & Morgan, D. Material Discovery and Design Principles for Stable, High Activity Perovskite Cathodes for Solid Oxide Fuel Cells. *Adv. Energy Mater.* **8**, 1702708 (2018).
2. Feng, M. & Goodenough, J. B. A superior oxide-ion electrolyte. *Eur. J. Solid State Inorg. Chem.* **31**, 663–72 (1994).
3. Sun, C., Alonso, J. A. & Bian, J. Recent Advances in Perovskite-Type Oxides for Energy Conversion and Storage Applications. *Adv. Energy Mater.* **11**, 1–21 (2021).
4. Larson, A. C. & Von Dreele, R. B. General Structure Analysis System (GSAS). *Los Alamos Natl. Lab. Rep. LAUR* 86–748 (1994).
5. Cherepanov, V. A., Filonova, E. A., Voronin, V. I. & Berger, I. F. Phase equilibria in the LaCoO_3 - LaMnO_3 - $\text{BaCoO}_{(z)}$ - BaMnO_3 system. *J. Solid State Chem.* **153**, 205–211 (2000).
6. Parsons, T. G., D'Hondt, H., Hadermann, J. & Hayward, M. A. Synthesis and structural characterization of $\text{La}_{1-x}\text{A}_x\text{MnO}_{2.5}$ ($A = \text{Ba, Sr, Ca}$) phases: Mapping the variants of the brownmillerite structure. *Chem. Mater.* **21**, 5527–5538 (2009).

5. 主な発表論文等

〔雑誌論文〕 計5件（うち査読付論文 5件/うち国際共著 5件/うちオープンアクセス 0件）

1. 著者名 Ka H Hong, Elena Solana-Madruga, Branislav Viliam Hakala, Midori Amano Patino, Pascal Manuel, Yuichi Shimakawa, J Paul Attfield	4. 巻 5
2. 論文標題 Substitutional tuning of electronic phase separation in CaFe3O5	5. 発行年 2021年
3. 雑誌名 Physical Review Materials	6. 最初と最後の頁 24406
掲載論文のDOI (デジタルオブジェクト識別子) 10.1103/PhysRevMaterials.5.024406	査読の有無 有
オープンアクセス オープンアクセスではない、又はオープンアクセスが困難	国際共著 該当する
1. 著者名 Anucha Koedtrud, Midori Amano Patino, Noriya Ichikawa, Daisuke Kan, Yuichi Shimakawa	4. 巻 286
2. 論文標題 Crystal structures and ionic conductivity in Li20HX (X= Cl, Br) antiperovskites	5. 発行年 2020年
3. 雑誌名 Journal of Solid State Chemistry	6. 最初と最後の頁 121263
掲載論文のDOI (デジタルオブジェクト識別子) 10.1016/J.JSSC.2020.121263	査読の有無 有
オープンアクセス オープンアクセスではない、又はオープンアクセスが困難	国際共著 該当する
1. 著者名 Denis Romero F, Amano Patino M, Haruta M, Kurata H, Attfield JP, Shimakawa Y	4. 巻 59(1)
2. 論文標題 Conversion of a Defect Pyrochlore into a Double Perovskite via High-Pressure, High-Temperature Reduction of Te6+	5. 発行年 2019年
3. 雑誌名 Inorganic Chemistry	6. 最初と最後の頁 343-349
掲載論文のDOI (デジタルオブジェクト識別子) 10.1021/acs.inorgchem.9b02472	査読の有無 有
オープンアクセス オープンアクセスではない、又はオープンアクセスが困難	国際共著 該当する
1. 著者名 Takafumi Yamamoto, Harry WT Morgan, Dihao Zeng, Takateru Kawakami, Midori Amano Patino, Michael A Hayward, Hiroshi Kageyama, John E McGrady	4. 巻 58(22)
2. 論文標題 Pressure-Induced Transitions in the 1-Dimensional Vanadium Oxyhydrides Sr2VO3H and Sr3V2O5H2, and Comparison to 2-Dimensional SrVO2H	5. 発行年 2019年
3. 雑誌名 Inorganic Chemistry	6. 最初と最後の頁 15393
掲載論文のDOI (デジタルオブジェクト識別子) 10.1021/acs.inorgchem.9b02459	査読の有無 有
オープンアクセス オープンアクセスではない、又はオープンアクセスが困難	国際共著 該当する

1. 著者名 Xabier Martinez de Irujo-Labalde, Masato Goto, Esteban Urones-Garrote, Ulises Amador, Clemens Ritter, Midori E Amano Patino, Anucha Koedtruad, Zhenhong Tan, Yuichi Shimakawa, Susana Garcia-Martin	4. 巻 31(15)
2. 論文標題 Multiferroism Induced by Spontaneous Structural Ordering in Antiferromagnetic Iron Perovskites	5. 発行年 2019年
3. 雑誌名 Chemistry of Materials	6. 最初と最後の頁 5993-6000
掲載論文のDOI (デジタルオブジェクト識別子) 10.1021/acs.chemmater.9b02716	査読の有無 有
オープンアクセス オープンアクセスではない、又はオープンアクセスが困難	国際共著 該当する

〔学会発表〕 計4件 (うち招待講演 1件 / うち国際学会 3件)

1. 発表者名 Midori Amano Patino*, Fabio Denis Romero, Masato Goto, Saito Takashi, Yuichi Shimakawa, Fabio Orlandi, Pascal Manuel, Paul Attfield, Yuichi Shimakawa
2. 発表標題 Unusual Field-dependent Magnetism of Square-planar Iron(II) Centres in CaFe ₃ Ti ₄ O ₁₂
3. 学会等名 Chemical Society of Japan (CSJ)
4. 発表年 2020年

1. 発表者名 Midori Amano Patino*, Fabio Denis Romero, Masato Goto, Saito Takashi, Yuichi Shimakawa
2. 発表標題 Synthesis and Characterization of the Quadruple Perovskite CaFe ₃ Ti ₄ O ₁₂ with Unusual Square-planar Fe ²⁺ Spin Ordering
3. 学会等名 Integrated Research Consortium on Chemical Sciences (IRCCS) (国際学会)
4. 発表年 2019年

1. 発表者名 Midori Amano Patino*, Fabio Denis Romero, Masato Goto, Saito Takashi, Yuichi Shimakawa
2. 発表標題 Unusual magnetic ordering and switching of iron spins at the A'-sites in CaFe ₃ Ti ₄ O ₁₂
3. 学会等名 Core-to-Core Symposium (国際学会)
4. 発表年 2019年

1. 発表者名 Midori Amano Patino*, Fabio Denis Romero, Masato Goto, Saito Takashi, Yuichi Shimakawa
2. 発表標題 Unusual magnetic spin ordering and switching of square-planar Fe ²⁺ in CaFe ₃ Ti ₄ O ₁₂
3. 学会等名 International Conference of Computational Methods in Sciences and Engineering (ICCMSE) (招待講演) (国際学会)
4. 発表年 2019年

〔図書〕 計0件

〔産業財産権〕

〔その他〕

-

6. 研究組織

氏名 (ローマ字氏名) (研究者番号)	所属研究機関・部局・職 (機関番号)	備考

7. 科研費を使用して開催した国際研究集会

〔国際研究集会〕 計0件

8. 本研究に関連して実施した国際共同研究の実施状況

共同研究相手国	相手方研究機関			
その他の国・地域	Taiwan NSRRC			
英国	University of Edinburg			
スペイン	Universidad Complutense of Madrid			